

Equilibrium Vacancy Concentration Driven by Undetectable Impurities

Thomas Schuler,* Caroline Barouh, Maylise Nastar, and Chu-Chun Fu
CEA, DEN, Service de Recherches de Métallurgie Physique, F-91191 Gif-sur-Yvette, France
(Received 11 February 2015; published 29 June 2015)

By means of *ab initio* calculations combined to statistical mechanics, we provide new evidence that an experimentally undetectable tiny amount of impurities can be responsible for drastic changes in vacancy concentrations ($[V]$), inducing large deviations from an Arrhenius law even at low temperature. It is the case of O and N in α -Fe. The present finding is fully compatible with existing experiments, and changes the previous common vision that C has the dominant effect. This study provides a route for bridging the longstanding theoretical-experimental gap on the prediction of $[V]$ in metals.

DOI: 10.1103/PhysRevLett.115.015501

PACS numbers: 61.72.J-, 05.70.-a, 61.72.S-, 71.15.Mb

Solid systems unavoidably contain structural defects and impurities. It is well known that there may be strong interactions between them, inducing drastic changes of thermodynamic and kinetic properties of the system. However, the physical processes involved are generally unclear and not accessible by experiments. In particular, residual interstitial impurities at concentrations below the limit of detection systematically remain in the so-called high-purity metallic samples. The simplest and the most common structural defect in metals is the vacancy (V), which mediates the atomic transport of substitutional elements and therefore the evolution of microstructures. However, fundamental properties of vacancies, such as their formation free enthalpy $G^f(V)$, which dictates the vacancy concentration at thermal equilibrium and acts as a main driving force for V elimination out of equilibrium, is poorly known in transition metals (e.g., Cr, Nb, Ni, Zr, Ti [1]). Among experimental difficulties is the sample contamination by impurities. Atomistic simulations may provide relevant insights beyond the experimental resolution, but in practice, these studies are usually limited to too idealized systems (e.g., Cr [2], W [3]). Thus, longstanding experimental-theoretical gaps exist for these elementary quantities. This is, for instance, the case of bcc iron, the basic component of steels.

In ferromagnetic α -Fe, there are only two measurements of the V formation enthalpy: $H^f = 1.66 \pm 0.1$ eV from muons spin rotation (μ SR) [4] and $H^f = 2.00 \pm 0.2$ eV from positron annihilation spectroscopy (PAS) in carbon-doped samples [5]. In the paramagnetic state, H^f is estimated between 1.40 and 2.00 eV [5–9]. These disparate results have led to a longstanding controversy about the interpretation of resistivity recovery experiments [10].

In iron, additional complexity stems from the magnetic transition. However a recent theoretical study based on density functional theory (DFT) calculations leads to a very good agreement with the experimental self-diffusion coefficient in α -Fe [11]. A semiphenomenological model is used to account for magnetic disordering effects using 3

parameters: the reduced magnetization (experimental value [12]), $G^f(V) = 2.13$ eV at $T = 0$ K (DFT calculation, in agreement with previous results within ± 0.1 eV [13–18]) and $G^f(V) = 1.98$ eV for fully magnetically disordered α -Fe. These $G^f(V)$ values are well above most experimental results but the fact that they allow a correct prediction of the self-diffusion coefficient [which is proportional to $G^f(V)$] makes them reliable, along with the simple magnetic model. The existence of another type of V population in the samples, essentially immobile and not contributing to the α -Fe self-diffusion coefficient, could explain the fact that experimental $G^f(V)$ are generally lower than theoretical values. Indeed, high-purity α -Fe samples always contain a few atomic part per million (appm) of C, N, and O atoms. Several experiments have pointed out that at such low concentrations, C and N may already have important effects on the V population in α -Fe [19–23]. These effects stem from an attractive binding between V and C or N, as confirmed by DFT calculations (see, e.g., Ref. [17] and references therein). Therefore, there are vacancy-solute clusters in the solid solution, and as the solutes are located in an off-centered position rather than inside the vacancy [17], muons and/or positrons are sensitive to the free space existing in these clusters [24] (cf., Fig. 1). This way, the experimental techniques mentioned above would measure the total V concentration in the

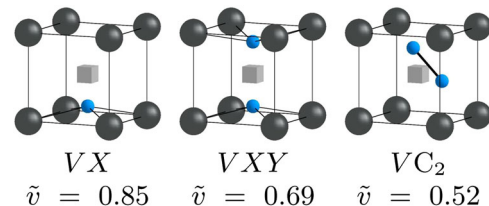


FIG. 1 (color online). Most stable cluster configurations. Gray spheres, gray squares, and blue spheres represent Fe atoms, V , and solutes, respectively. \tilde{v} is the Voronoï volume of V (free space inside V), normalized by the Voronoï volume of the isolated V (10.9 \AA^3).

sample, $[V]$, not the isolated V concentration. It is now well known that some solute atoms (e.g., H) are able to increase the equilibrium $[V]$ [25–29]. Thus the effective vacancy formation free enthalpy in the solid solution containing impurities ($G^f(V)_{|\text{Fe-CNO}}$) might be much lower than in pure α -Fe ($G^f(V)_{|\text{Fe}}$), the theoretical DFT value. V - X binding energies are quite high in α -Fe [17,30–32], and could be able to balance the low solute concentrations.

De Schepper *et al.* [5] have shown that VC pairs need to be taken into account in their analysis of PAS data. They obtained $H^f = 2.0 \pm 0.2$ eV in ferromagnetic α -Fe, which is higher than previous estimations, and closer to DFT results. Neglecting these VC pairs, they get a much lower “effective” value: $H^f = 1.56 \pm 0.1$ eV.

DFT results provide some new insights because it is known that N and O have a higher binding with V than C. Moreover, VX_2 clusters are particularly stable [17,30,33,34]. Ultimately, which are the vacancy-solute clusters mainly responsible for the lowering of $G^f(V)_{|\text{Fe-CNO}}$?

To answer this question, we present a model of effective vacancy formation free enthalpy for multicomponent dilute alloys applied to an α -Fe matrix containing C, N, and O atoms. This model relies on a low-temperature expansion (LTE) of the partition function [17,35–37]. As Monte Carlo methods [38–40] are not suited for the study of dilute solid solutions [17], this LTE formalism provides an accurate way of bridging the gap between Lomer’s model for infinitely dilute solid solutions [41] and the cluster-variation method for concentrated alloys [42,43]. Our results enable a reinterpretation of μ SR and PAS experiments in ferromagnetic α -Fe.

In very dilute solid solutions, equilibrium cluster distributions are equally obtained from one of the various mass balance methods [25,33,44,45]. Nevertheless, the LTE method applied in our study can be rigorously generalized to more concentrated alloys. The partition function of the system is developed around a reference state, keeping in the series the excited states of lowest energies only. Using the linked-cluster theorem, one can express the semigrand-canonical free energy per lattice site of the system and deduce the total chemical species concentrations. Considering an α -Fe solid solution with C, N, and O atoms and vacancies, the following system must be solved:

$$\begin{aligned} [V] &= \sum_j n_j g_j \exp\left(\frac{\lambda_j}{kT}\right), \\ [X] &= \sum_j m_j(X) g_j \exp\left(\frac{\lambda_j}{kT}\right), \end{aligned} \quad (1)$$

with

$$\lambda_j = E^{bt}(j) + \sum_{\eta=\text{C,N,O}} m_j(\eta) \mu_\eta + n_j \mu_{V\text{Fe}}. \quad (2)$$

$X = \text{C, N or O}$ [meaning that Eq. (1) consists of four equations], j stands for a given configuration of the system, g_j is the number of equivalent configurations j (configurational entropy contribution), $E^{bt}(j)$ is the energy difference between configuration j and each component of j being isolated in the reference state, $m_j(\eta)$ and n_j are, respectively, the number of η atoms and the number of V in configuration j , μ_η is the difference between the chemical potentials of an atom η and an empty octahedral site, $\mu_{V\text{Fe}}$ is the difference between the chemical potentials of a substitutional empty site (V) and an Fe atom, and k stands for the Boltzmann constant. In the sums of Eq. (1), each term is interpreted as the concentration of a particular vacancy-solute cluster.

Using our DFT-based Hamiltonian [17], a comprehensive study including numerous clusters led us to the conclusion that VX and VX_2 clusters only need to be considered because they are the only ones that have a significant impact on $[V]$ in α -Fe- X stable (i.e., with solute concentrations below solubility limits) solid solutions at thermal equilibrium.

For each given solute concentration, vacancies are assumed to reach their equilibrium concentration by elimination and creation at perfect sinks, meaning that $\mu_{V\text{Fe}}$ is imposed. $\mu_{V\text{Fe}}$ is easily found considering that the isolated V concentration should correspond to the equilibrium one in pure Fe, $[V_{eq}]_{|\text{Fe}} = \exp(-G^f(V)_{|\text{Fe}}/kT) = \exp(\mu_{V\text{Fe}}/kT)$. The effect of magnetic disordering is taken into account via the semiempirical model that was proven efficient in the study of α -Fe self-diffusion [11], leading to a temperature-dependent expression of $G^f(V)_{|\text{Fe}}$:

$$\begin{aligned} G^f(V)_{|\text{Fe}} &= H_P^f + (H_F^f - H_P^f) M_0(T)^2 \\ &\quad - T[S_P^f + (S_F^f - S_P^f) M_0(T)^2]. \end{aligned} \quad (3)$$

H^f and S^f denote the vacancy formation enthalpy and entropy, while the F and P subscripts indicate the ferro- and paramagnetic state, respectively. M_0 is the reduced magnetization, its variation with temperature being obtained from experimental work [12]. $H_F^f = 2.12$ eV [17] and $H_P^f = 1.98$ eV [11] were computed using DFT. The values for $S_F^f \simeq 5k$ and $S_P^f \simeq 4k$ are taken from spin-lattice dynamics simulations [46], in agreement with previous DFT estimations of $S_F^f = 4.1k$ [15]. Our DFT calculations ($T = 0$ K) of H_F^f under strain show that the thermal expansion of the α -Fe matrix reduces H_F^f by less than 0.02 eV, which we will neglect.

The DFT binding energies of vacancy-solute clusters in the ferromagnetic state [17] are summarized in Table I. The binding energy of heterogeneous clusters (XY and VXY type, X and Y being two different solutes) were computed to investigate possible synergetic effects between C, N, and

TABLE I. Total binding energies (E^{bt}) and geometrical multiplicity (g) of $V-X$ clusters included in the LTE. The most stable configurations are pictured in Fig. 1. They are all similar except for the VC_2 cluster: an alternative, slightly more stable configuration exists (“ VC_2 ” configuration).

		VX	VCX	VNX	VOX
$X = C$	E^{bt}	0.41	1.18	1.18	1.88
	g	6	12	6	6
$X = N$	E^{bt}	0.73	1.18	1.56	2.26
	g	6	6	3	6
$X = O$	E^{bt}	1.43	1.88	2.26	2.97
	g	6	6	6	3

O. Figure 1 shows the most stable configurations of VX and VXY clusters.

At fixed solute concentration, as temperature increases, vacancy-solute clusters tend to dissociate more often and the stabilizing effect of solutes decreases: $G^f(V)_{|Fe-X}$ increases. At fixed temperature, as the solute content increases, vacancy-solute clusters are more likely to appear and the stabilizing effect of solutes increases: $G^f(V)_{|Fe-X}$ decreases. $G^f(V)_{|Fe-X}$ is first investigated as a function of temperature when the solute content equals the solubility limit (see Fig. 2): as temperature increases, the solute content increases as well, leading to a competition between these two parameters. The calculation of the solid solution solubility limits at equilibrium with an ordered phase is detailed in Ref. [17].

Table I shows that $E^{bt}(VC) < E^{bt}(VN) < E^{bt}(VO)$. Solubility limits compare differently: $[O]_T^{sol} < [C]_T^{sol} < [N]_T^{sol}$. The competition between these two parameters

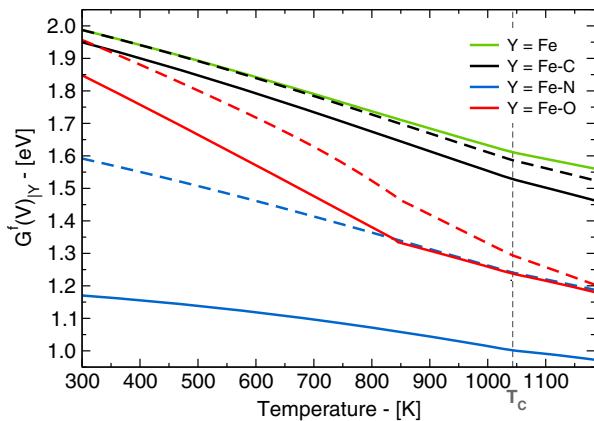


FIG. 2 (color online). Effective V formation free enthalpy as a function of temperature: the solid green line is $G^f(V)_{|Fe}$. The black, blue, and red lines represent $G^f(V)_{|Fe-X}$ when $[X] = [X]_T^{sol}$, X being, respectively, C, N, and O. For these three, dashed lines are obtained using only VX pairs in our calculations, while solid lines are obtained considering VX as well as VX_2 clusters.

explains Fig. 2. For O, the slope change at $T = 843$ K relates to the fact that the most stable Fe oxide changes from Fe_3O_4 to FeO at this temperature. If each solute is at its respective solubility limit, whatever T , $G^f(V)_{|Fe-N} < G^f(V)_{|Fe-O} < G^f(V)_{|Fe-C}$. We should, however, emphasize the fact that $[O]_T^{sol}$ varies from 10^{-24} to 10^{-6} between 300 K and 1000 K, meaning that $[O]$ cannot be precisely measured experimentally. If VX pairs only are included in the calculation, then the solute effect on $G^f(V)_{|Fe-X}$ is underestimated (dashed lines in Fig. 2). Even if the solid solution is very dilute, VX_2 clusters must be considered because of their high binding energy. This feature should be taken into account in the analysis of experimental results.

In ferromagnetic α -Fe, vacancy concentrations are too low to be measured by PAS experiments. Yet, De Schepper *et al.* [5] succeeded by doping the sample with C to increase $[V]$, as it was known that positrons were also trapped by VC pairs. In Ref. [5], the Fe sample has the following impurity content: $[C] \leq 1$ appm, $[N] \leq 0.2$ appm, $[O] \leq 0.5$ appm. Since our calculation shows that C has a small effect on $G^f(V)$, we propose a reinterpretation of this experiment, as well as guidelines for future experimental work.

Figure 3 shows the temperature variation of $G^f(V)_{|Fe-CNO}$ obtained from LTE with various impurity contents. The green curve corresponds to pure α -Fe [Eq. (3)]. The other curves all have a similar shape: $G^f(V)_{|Fe-CNO}$ increases at low temperature because $[N] < [N]_T^{sol}$, so as temperature increases the concentration of $V-N$ clusters decreases, while C and O do not significantly affect $G^f(V)_{|Fe-CNO}$. At $T \approx 450$ K, there is a maximum because $[O]_T^{sol}$ (hence $[O]$ in the solid solution) becomes sufficiently high to lower $G^f(V)_{|Fe-CNO}$. For 400 K $< T < 500$ K, there is a small effect of heterogeneous clusters: $G^f(V)_{|Fe-CNO}$ would be about 0.02 eV

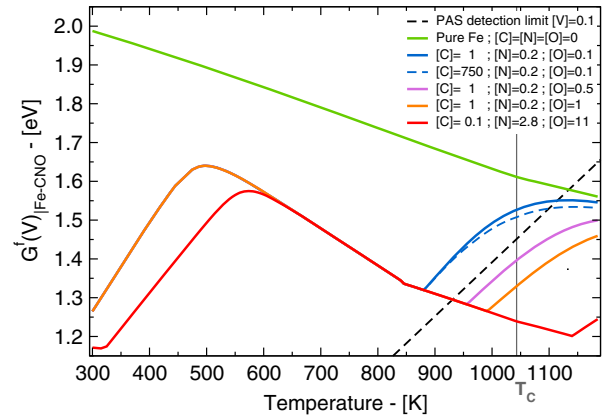


FIG. 3 (color online). Calculated $G^f(V)_{|Fe-CNO}$ as a function of temperature with various nominal impurity contents (in appm). The solute content in the solid solution is $\min([X]; [X]_T^{sol})$. The black dashed line corresponds to an estimated PAS detection threshold, $G^f(V)_{min}$ [47].

higher without VXY clusters ($X \neq Y$), or in other words, $[V]$ would be about 1.5 times lower. XY clusters are slightly attractive but they have no influence on the results. Then, up to 850–1100 K (depending on the O nominal content), $G^f(V)_{\text{Fe-CNO}} \approx G^f(V)_{\text{Fe-O}}$ with $[O] = [O]_T^{\text{sol}}$ (cf. Fig. 2). Despite very low O solubility limits, this species controls $[V]$ in high purity α -Fe. Once $[O] < [O]_T^{\text{sol}}$, the concentration of $V-O$ clusters decreases and $G^f(V)_{\text{Fe-CNO}}$ increases with increasing temperature. High C content might slightly reduce $G^f(V)$ for this temperature range (dashed blue curve).

Seeger [47] estimated the minimum vacancy concentration detectable from PAS experiments: $[V]_{\text{min}} = \exp(-G^f(V)_{\text{min}}/kT) \approx 10^{-7}$ (dashed black curve in Fig. 3). Vacancy concentrations are thus measurable using PAS if $G^f(V)_{\text{Fe-CNO}} < G^f(V)_{\text{min}}$.

From our calculations, we understand that this condition is fulfilled, not because of C atoms but because of O atoms, with $[O] = [O]_T^{\text{sol}} \approx 0.1$ –1 appm. The original interpretation of the results (VC pair effect) requires a much higher $V-C$ binding energy than what DFT values suggest [17]. A small O contamination of the sample (about 0.1–1 appm) during the C-doping procedure would increase $[V]$: it is thus an alternative explanation to the PAS results from Ref. [5]. To confirm this interpretation, O concentrations should always be measured, despite experimental difficulties, before and after PAS experiments to detect any O contamination of the sample. Finally, the analysis of PAS results should take into account the fact that not only VX pairs are able to trap positrons, but also VX_2 clusters. Indeed Fig. 2 demonstrates that the proportion of vacancies belonging to these VX_2 clusters is substantial.

Fürderer *et al.* [4] have measured $G^f(V)$ in ferromagnetic α -Fe using the μ SR technique: $G^f(V) = 1.66 \pm 0.07 - (1.64 \pm 0.67)kT$ eV. The sample impurity contents are assumed to be constant during the μ SR experiment and equal to: $[C] = 0.1$ appm, $[N] = 2.8$ appm, $[O] = 11$ appm [48]. It is also assumed that $G^f(V)_{\text{Fe}} = H^f - TS^f$, H^f and S^f being constant over the whole temperature range. The muon relaxation rate Γ is measured as a function of temperature and $G^f(V)_{\text{Fe}}$ is deduced from the relation: $-kT \ln \Gamma = [H^f + E^m(\mu)] - T(k \ln \sigma_0 + S^f)$, with $\sigma_0 \exp(-E^m(\mu)/kT)$ being the trapping rate of a muon into a monovacancy.

The entropy value deduced from this experiment (S^f) is not very trustful because in the equation it is combined with modeling parameters (σ_0) that are not well established. The enthalpy (H^f) is more trustful since $E^m(\mu) \approx 0.04$ eV $\ll H^f$. Finally, the measure does not correspond to $G^f(V)_{\text{Fe}}$ but to an effective value weighted by the sensitivity of muons to V , VX , and VX_2 .

We performed the multicomponent calculation (solid solution including simultaneously C, N, and O solutes) at

concentrations which are the lowest among the ones given in Ref. [4] and $[X]_T^{\text{sol}}$. Assuming that $G^f(V)_{\text{Fe-CNO}}$ varies linearly with temperature and that muons respond in the same way to isolated V and vacancy-solute clusters, we extrapolate H^f from our results in the narrow temperature range where the μ SR experiment is conducted (925 K $< T < 1000$ K). This approach mimics the experimental one and we get $H^f_{\text{Fe-CNO}} = 1.75$ eV, in rather good agreement with the experimental value ($H^f = 1.66 \pm 0.07$). If we consider isolated V only, a higher value is obtained: $H^f_{\text{Fe}} = 2.15$ eV.

In paramagnetic α -Fe ($T > 1043$ K), the curves in Fig. 3 show that the calculation of H^f with a similar procedure would give results that are very dependent on the O content and the temperature range where the experiment is performed, which could explain the rather large discrepancy between various measurements [5–9].

Calculations performed under various DFT implementations (using different exchange-correlation functionals, pseudopotentials, and basis sets) give binding energies within ± 0.15 eV, the deviations between two implementations having the same sign and magnitude for each cluster and solute. At $T > 900$ K, the subsequent error bar on $G^f(V)_{\text{Fe-CNO}}$ is ≤ 0.15 eV, and our results remain qualitatively unchanged.

Whatever the temperature evolution of $V-X$ binding energies and/or $G^f(V)_{\text{Fe}}$, the above calculations show an important decrease of the effective V formation free enthalpy in α -Fe solid solutions due to the presence of interstitial solutes, especially N and O, C having little influence, at variance with previous studies [5,49]. It seems that accounting for the presence of O impurities in Fe samples in very low concentrations ($\ll 1$ appm, i.e., below detection threshold) allows us to quantitatively reproduce experimental $G^f(V)_{\text{Fe}}$ in ferromagnetic α -Fe [4,5] from DFT data. It would be interesting to perform these experiments again, paying particular attention to the O concentration, the effect of VX_2 clusters, and the nonlinear variation of $G^f(V)_{\text{Fe-CNO}}$ with temperature.

The μ SR and PAS experiments could also be used as indirect measurements of the $[O]$ solubility limit and/or $V-O$ binding energies, quantities for which reliable experimental data are still lacking, while of practical importance to understand Fe oxidation and phenomena involving vacancies in α -Fe. The driving force for V elimination in out-of-equilibrium systems [50–54] depends on the excess vacancy concentration with respect to the equilibrium $[V]$. Even in high-purity Fe, V driving forces will be systematically overestimated because, as we have shown, interstitial solutes increase $[V]$ at thermal equilibrium. Moreover, some functional properties [55–57] and the kinetics of many processes based on vacancy-mediated diffusion [51,58,59] also depend on the quantity of vacancy-solute clusters.

To improve the quantitiveness of the calculation, further studies on the temperature and magnetic effects on clusters binding energies are required. The results will be easily included in the analytical expressions derived in this Letter. These expressions are straightforward to apply in other relevant materials, e.g., transition metals rare earth oxides [60], AlZr [61], ZrNb [62], FeCr [63], or NiC [64–66]. A striking feature highlighted in this Letter which should occur in many systems is the nonlinearities of the effective vacancy formation free enthalpy, within temperature ranges for which it is conventionally admitted that an Arrhenius law is valid. It is due to the combined effect of various impurities, each one affecting the vacancy concentration on a specific temperature range depending both on its binding energy with vacancies and on its concentration.

This work was supported by the joint program “CPR ODISSEE” funded by AREVA, CEA, CNRS, EDF and Mécachrome under Contract No. 070551. DFT calculations were performed using resources from IFERC-CSC (SISteel) and GENCI (x2015096020).

*Corresponding author.
thomas.schuler@cea.fr

- [1] Landolt and Bornstein, *Atomic Defects in Metals*, Numerical Data and Functional Relationships in Science Technology - Group III: Crystal and Solid State Physics (Springer-Verlag, Berlin, 1991), Vol. 25.
- [2] R. Soulaïrol, C.-C. Fu, and C. Barreateau, *Phys. Rev. B* **83**, 214103 (2011).
- [3] L. Ventelon, F. Willaime, C.-C. Fu, M. Heran, and I. Ginoux, *J. Nucl. Mater.* **425**, 16 (2012).
- [4] K. Fürderer, K.-P. Döring, M. Gladisch, N. Haas, D. Herlach, J. Major, H.-J. Mundinger, J. Rosenkranz, W. Schäfer, L. Schimmele, M. Schmoltz, W. Schwartz, and A. Seeger, *Hyperfine Interact.* **31**, 81 (1986).
- [5] L. De Schepper, D. Segers, L. Dorikensvanpraet, M. Dorikens, G. Knuyt, L.M. Stals, and P. Moser, *Phys. Rev. B* **27**, 5257 (1983).
- [6] H. E. Schaefer, K. Maier, M. Weller, D. Herlach, A. Seeger, and J. Diehl, *Scr. Metall.* **11**, 803 (1977).
- [7] S. M. Kim and W. J. L. Buyers, *J. Phys. F* **8**, L103 (1978).
- [8] H. Matter, J. Winter, and W. Triftshäuser, *J. Appl. Phys.* **20**, 135 (1979).
- [9] Y. Shirai, H. E. Schaefer, and A. Seeger, *Positron Annihilation* (World Scientific Publishing Co., Singapore, 1989), pp. 419–421.
- [10] O. Seydel, G. Froberg, and H. Wever, *Phys. Status Solidi A* **144**, 69 (1994).
- [11] H. Ding, V. I. Razumovskiy, and M. Asta, *Acta Mater.* **70**, 130 (2014).
- [12] J. Crangle and G. M. Goodman, *Proc. R. Soc. A* **321**, 477 (1971).
- [13] C. Domain and C. S. Becquart, *Phys. Rev. B* **65**, 024103 (2001).
- [14] F. Soisson and C.-C. Fu, *Phys. Rev. B* **76**, 214102 (2007).
- [15] G. Lucas and R. Schäublin, *Nucl. Instrum. Methods Phys. Res., Sect. B* **267**, 3009 (2009).
- [16] D. Kandaskalov, C. Mijoule, and D. Connétable, *J. Nucl. Mater.* **441**, 168 (2013).
- [17] C. Barouh, T. Schuler, C.-C. Fu, and M. Nastar, *Phys. Rev. B* **90**, 054112 (2014).
- [18] L. Messina, M. Nastar, T. Garnier, C. Domain, and P. Olsson, *Phys. Rev. B* **90**, 104203 (2014).
- [19] F. E. Fujita and A. C. Damask, *Acta Metall.* **12**, 331 (1964).
- [20] M. Wuttig, J. T. Stanley, and H. K. Beirnbäum, *Phys. Status Solidi* **27**, 701 (1968).
- [21] A. Vehanen, P. Hautojärvi, J. Johansson, J. Yli-Kaupilla, and P. Moser, *Phys. Rev. B* **25**, 762 (1982).
- [22] S. Takaki, J. Fuss, H. Kuglers, U. Dedek, and H. Schultz, *Radiat. Eff.* **79**, 87 (1983).
- [23] A. L. Nikolaev and T. E. Kurenykh, *J. Nucl. Mater.* **414**, 374 (2011).
- [24] D. Terentyev, K. Heinola, A. Bakaev, and E. E. Zhurkind, *Scr. Mater.* **86**, 9 (2014).
- [25] L. Ismer, M. S. Park, A. Janotti, and C. G. Van de Walle, *Phys. Rev. B* **80**, 184110 (2009).
- [26] Y.-L. Liu, H.-B. Zhou, Y. Zhang, and C. Duan, *Comput. Mater. Sci.* **62**, 282 (2012).
- [27] M. L. Fullarton, R. E. Voskoboïnikov, and S. C. Middleburgh, *J. Alloy Comp.* **587**, 794 (2014).
- [28] S. Hidehiko and F. Yuh, *Acta Mater.* **67**, 418 (2014).
- [29] D. Tanguy, Y. Wang, and D. Connétable, *Acta Mater.* **78**, 135 (2014).
- [30] C. Domain, C. S. Becquart, and J. Foct, *Phys. Rev. B* **69**, 144112 (2004).
- [31] C. L. Fu, M. Krcmar, G. S. Painter, and X.-Q. Chen, *Phys. Rev. Lett.* **99**, 225502 (2007).
- [32] Y. Jiang, J. R. Smith, and G. R. Odette, *Phys. Rev. B* **79**, 064103 (2009).
- [33] C.-C. Fu, E. Meslin, A. Barbu, F. Willaime, and V. Oison, *Solid State Phenom.* **139**, 157 (2008).
- [34] A. T. Paxton and C. Elsässer, *Phys. Rev. B* **87**, 224110 (2013).
- [35] M. F. Sykes, D. S. Gaunt, J. W. Essam, and D. L. Hunter, *J. Math. Phys. (N.Y.)* **14**, 1060 (1973).
- [36] F. Ducastelle, *Order and Phase Stability in Alloys* (North-Holland, 1991).
- [37] E. Clouet and M. Nastar, *Phys. Rev. B* **75**, 132102 (2007).
- [38] J. Mayer and M. Fahnle, *Acta Mater.* **45**, 2207 (1997).
- [39] A. Van der Ven and G. Ceder, *Phys. Rev. B* **71**, 054102 (2005).
- [40] A. Biborski, L. Zosiak, R. Kozubski, R. Sot, and V. Pierron-Bohnes, *Intermetallics* **18**, 2343 (2010).
- [41] W. M. Lomer, *Vacancies and Other Point Defects in Metals and Alloys* (Institute of Metals, London, 1958), pp. 79–98.
- [42] R. Kikuchi, *Phys. Rev.* **81**, 988 (1951).
- [43] M. Nastar and F. Soisson, *Phys. Rev. B* **86**, 220102 (2012).
- [44] S. B. Zhang and J. E. Northrup, *Phys. Rev. Lett.* **67**, 2339 (1991).
- [45] C. J. Först, J. Slycke, K. J. Van Vliet, and S. Yip, *Phys. Rev. Lett.* **96**, 175501 (2006).
- [46] H. Wen, P.-W. Ma, and C. H. Woo, *J. Nucl. Mater.* **440**, 428 (2013).
- [47] A. Seeger, *Phys. Status Solidi A* **167**, 289 (1998).

- [48] J. Major, K. Fürderer, and D. Herlach, *Rev. Sci. Instrum.* **56**, 1428 (1985).
- [49] R. B. McLellan and M. L. Wasz, *Phys. Status Solidi A* **110**, 421 (1988).
- [50] S. Pogatscher, H. Antrekowitsch, M. Werinos, F. Moszner, S. S. A. Gerstl, M. F. Francis, W. A. Curtin, J. F. Löffler, and P. J. Uggowitzer, *Phys. Rev. Lett.* **112**, 225701 (2014).
- [51] M. Nastar and F. Soisson, *Comp. Nucl. Mater.* **1**, 471 (2012).
- [52] S. Moll, T. Jourdan, and H. Lefaix-Jeuland, *Phys. Rev. Lett.* **111**, 015503 (2013).
- [53] M. Herbig, D. Raabe, Y. J. Li, P. Choi, S. Zaefferer, and S. Goto, *Phys. Rev. Lett.* **112**, 126103 (2014).
- [54] Y. Li, D. Raabe, M. Herbig, P.-P. Choi, S. Goto, A. Kostka, H. Yarita, C. Borchers, and R. Kirchheim, *Phys. Rev. Lett.* **113**, 106104 (2014).
- [55] E. H. Khan, M. H. Weber, and M. D. McCluskey, *Phys. Rev. Lett.* **111**, 017401 (2013).
- [56] N. A. Richter, S. Siculo, S. V. Levchenko, J. Sauer, and M. Scheffler, *Phys. Rev. Lett.* **111**, 045502 (2013).
- [57] G. E. Murgida and M. V. Ganduglia-Pirovano, *Phys. Rev. Lett.* **110**, 246101 (2013).
- [58] D. Caliste and P. Pochet, *Phys. Rev. Lett.* **97**, 135901 (2006).
- [59] T. Garnier, V. R. Manga, D. R. Trinkle, M. Nastar, and P. Bellon, *Phys. Rev. B* **88**, 134108 (2013).
- [60] M. V. Ganduglia-Pirovano, A. Hofmann, and J. Sauer, *Surf. Sci. Rep.* **62**, 219 (2007).
- [61] S. Özbilen and H. M. Flower, *Acta Metall.* **37**, 2993 (1989).
- [62] X. K. Xin, W. S. Lai, and B. X. Liu, *J. Nucl. Mater.* **393**, 197 (2009).
- [63] A. P. Druzhkov and A. L. Nikolaev, *J. Nucl. Mater.* **408**, 194 (2011).
- [64] J. Wolff, M. Franz, J.-E. Kluin, and D. Schmid, *Acta Mater.* **45**, 4759 (1997).
- [65] D. J. Hepburn, D. Ferguson, S. Gardner, and G. J. Ackland, *Phys. Rev. B* **88**, 024115 (2013).
- [66] H. Z. Fang, S. L. Shang, Y. Wang, Z. K. Liu, D. Alfonso, D. E. Alman, Y. K. Shin, C. Y. Zou, A. C. T. van Duin, Y. K. Lei, and G. F. Wang, *J. Appl. Phys.* **115**, 043501 (2014).